2025 IEEE International Conference on Systems, Man, and Cybernetics (SMC)
October 5-8, 2025. Vienna, Austria

Shapelet Temporal Evolution Graph Network for Water Quality Anomaly Detection

Xiangxi Wu[1], Jing Bi[1,2], Gongming Wang[1,2], Ziqi Wang[3], Yibo Li[1], Junqi Zhang[1], Haitao Yuan[4], Jia Zhang[5] and Xingyang Chang[6]

[1]College of Computer Science, Beijing University of Technology, Beijing 100124, China
[2]Beijing Laboratory of Smart Environmental Protection, Beijing University of Technology, Beijing, China
[3]School of Software Technology, Zhejiang University, Ningbo 315100, China
[4]School of Automation Science and Electrical Engineering, Beihang University, Beijing 100191, China
[5]Dept. of Computer Science in Lyle School of Engineering, Southern Methodist University, Dallas, TX, USA
[6]School of Artificial Intelligence, Beijing University of Posts and Telecommunications, Beijing 100876, China

2025 IEEE International Conference on Systems, Man, and Cybernetics (SMC) | 979-8-3315-3358-8/25/$31.00 ©2025 IEEE | DOI: 10.1109/SMC58881.2025.11342887

***Abstract*—Water quality anomaly detection refers to the identification of abnormal changes in water parameters, which is crucial for ensuring environmental safety and preventing contamination events. With the growing volume of water environment sensing data and increasing demand for intelligent, transparent water quality management systems, achieving accurate, rapid, and interpretable anomaly detection has become a critical challenge in early warning systems. To tackle this challenge, this work proposes an anomaly detection model named Shapelet Temporal Evolution Graph Network (STEG), which constructs time-aware Shapelets and adopts graph attention networks to build Shapelets evolution graphs, learning multidimensional dynamic relationships within and between time segments. By incorporating both local and global temporal evolution factors, the approach ensures the interpretability of both the detection process and its resulting outputs. Experiments on two real-world datasets show that STEG outperforms state-of-the-art methods in terms of anomaly detection accuracy and generalization. Moreover, it provides clear and transparent reasoning for water quality anomaly detection.**

***Index Terms*—Anomaly detection, time series modeling, time-aware Shapelets, and graph attention networks.**

I. INTRODUCTION

The aquatic ecological environment is increasingly threatened by pollution, climate change, and human activities, leading to unpredictable water quality fluctuations. Water quality anomaly detection aims to identify abnormal variations in water parameters, enabling early warning and source-tracing analysis to mitigate environmental risks and prevent large-scale contamination events. Water quality anomaly detection methods [1] can be divided into two categories: model-driven methods and data-driven methods.

Model-driven methods have been widely applied in water quality monitoring due to their reliability and interpretability. Researchers build models based on physical and chemical principles to simulate water behavior and predict quality changes. However, these models require numerous parameter inputs and a deep understanding of water dynamics, and the complexity of environmental factors as well as the difficulty of obtaining key parameters can affect their accuracy, limiting applicability in real-world environments. In contrast, data-driven methods reduce the reliance on specialized environmental knowledge by combining historical water quality data with statistical analysis, machine learning, and deep learning techniques to detect anomalies. Statistical techniques perform well in identifying trends and patterns but have limitations in capturing nonlinear relationships and handling complex data. To address these limitations, machine learning-based methods have emerged, which can handle high-dimensional inputs and model nonlinear relationships. However, they still struggle with capturing intricate spatial and temporal patterns, especially in large-scale or complex datasets.

In response to these challenges, deep learning techniques offer unique advantages. They excel at handling spatial and temporal water quality data, automatically extracting complex patterns from raw data. With their ability to learn features and handle high-dimensional data, deep learning provides an effective solution to the limitations of traditional machine learning methods. However, despite their advantages, these methods still have notable limitations. They rely heavily on the distribution of historical data and are vulnerable to outliers and noise, which can degrade model performance. Furthermore, their ability to generalize to new or unseen datasets can be limited. Moreover, due to their black-box nature, most deep learning models present challenges in interpreting the reasons behind their predictions.

Based on the aforementioned analysis, this work enhances anomaly detection accuracy and improves the interpretability of pollution source information. This is achieved by strengthening the detection capability of water quality early warning models and improving reasoning transparency through interpretable feature learning. A water quality anomaly detection model based on time-aware Shapelet and graph attention networks, named Shapelet Temporal Evolution Graph Network (STEG), is proposed. It incorporates interpretable learning of temporal and contextual features. By constructing time-

This work was supported by the National Natural Science Foundation of China under Grants 62473014 and 62173013, the Beijing Natural Science Foundation under Grants L233005 and 4232049, and in part by Beihang World TOP University Cooperation Program. (Corresponding author: Junqi Zhang.)

aware Shapelets and using graph attention networks to build Shapelet evolution graphs, STEG learns multidimensional dynamic relationships among segments. Furthermore, the integration of local and global factors within time-aware Shapelets guarantees the interpretability of both the reasoning process and its outputs.

The remaining sections of this work are organized as follows. Section II reviews the related work on anomaly detection methods. Section III describes the components and overall architecture of the proposed STEG model. Section IV introduces experimental datasets and presents a detailed discussion of the results. Finally, Section V concludes the work and outlines future research directions.

II. Related Work

Water quality anomaly detection has been widely studied. Traditional approaches primarily rely on statistical models, with Auto-Regressive Integrated Moving Average (ARIMA) [2] being one of the most commonly used. However, these methods generally rely on assumptions of linearity and stationarity, making them inadequate for modeling the complex nonlinear relationships commonly found in real-world water environments. To address these limitations, machine learning methods including Gradient Boosting Decision Trees (GBDT) [3] have been applied to water quality assessment and anomaly detection. These approaches perform well in modeling nonlinear relationships and handling high-dimensional data. However, they still face challenges in capturing temporal dependencies and spatial variations.

To further enhance the modeling capability under complex environmental conditions, deep learning methods have been adopted in anomaly detection tasks. Zhang *et al.* [4] propose ShapeEvoNet, a shapelet-based time series classification method that jointly performs shapelet extraction and evolutionary pattern learning in an end-to-end manner using a dilated causal CNN and a cluster evolution triplet loss. Duan *et al.* [5] propose ARISE, a graph anomaly detection framework that identifies topological and attribute anomalies by detecting dense substructures and employing graph contrastive learning to enhance node representation. Yuan *et al.* [6] propose MADG, a motif-level anomaly detection framework that combines motif-augmented GCN and temporal self-attention to capture both topological and temporal patterns of evolving substructures.

III. Model Framework

A. Overall architecture of STEG

Fig. 1 illustrates the structure of STEG. It mainly consists of the Shapelets candidate segment pool module, the time-aware Shapelets extraction module, and the Shapelets evolution graph construction module. Specifically, STEG extracts Shapelet segments from the time series, performs initial screening and constructs the candidate pool based on predefined rules. Next, the time-aware Shapelets extraction module captures the varying emphasis of Shapelets across time while reducing their number to ensure representativeness. Then, the Shapelets evolution graph construction module utilizes graph attention networks to uncover the evolutionary patterns between time-aware Shapelets. Finally, the representation learning module inputs the graph embedding features from the time-aware Shapelets evolution graph into an external classifier for anomaly detection of water quality indicators.

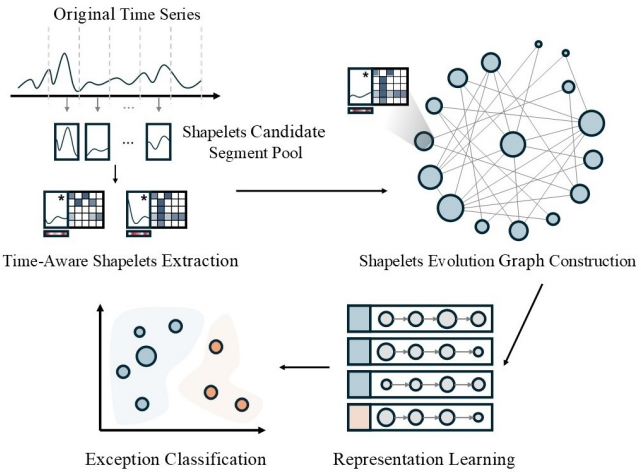

Fig. 1. Architecture of STEG

B. Shapelets candidate pool

Water quality monitoring data consists of long-term univariate time series, from which multiple Shapelet segments can be extracted. Data visualization and preliminary analysis reveal that variations in water quality indicators follow specific periodic patterns, with certain time segments exhibiting similar trends. Consequently, the Shapelets extracted from the entire time series also display similar patterns. STEG constructs a Shapelet candidate pool based on the original time series to minimize computational costs while improving model efficiency and extracting the most representative water quality variation patterns. Algorithm 1 shows the candidate Shapelets selection process from all possible subsequences, prioritizing those that maximize the pairwise distance between the extracted segments.

C. Time-aware shapelets extraction

The traditional definition of Shapelets [7] captures only the basic shape information of a segment. This work extends this definition by incorporating the representational capacity of Shapelets across different time periods. To capture the temporal similarities of Shapelets across different time intervals, this work introduces time-aware Shapelets. Building on the traditional Shapelets definition, two additional parameters, local factor w and global factor u, are introduced to quantitatively assess the temporal sensitivity of different Shapelets.

The local factor w represents the internal importance of each element within a Shapelet, indicating the extent to which an element contributes to the overall Shapelet characteristics.

Algorithm 1 Shapelets Candidate Generation Algorithm

Input: Time series (T), subsequence length (l), target number of Shapelets (K), candidate Shapelets set (C)
Output: Final Shapelets candidate

```
Initialize candidate Shapelets set C
Initialize subsequence set seq by extracting all subsequences of length l from T
Initialize dist as a zero vector of length size seq
for k=1:K do
    if k==1 then
        i=0
    else
        Find index i of the maximum value in dist
    end if
    Add seq[i] to C
    dist[i]= − 1
    Define N as the index set of seq containing values not equal to -1
    for each j in N do
        Compute Euclidean distance between seq[j] and seq[i]
        Update dist[j] with the computed sum
    end for
end for
Return C
```

The distance between a Shapelet v and a segment s is calculated as:

$$\begin{aligned}\hat{d}(v,s|w)&=\tau(v,s|a^*,w)\\&=\left(\sum_{k=1}^{p} w_{a_1^*(k)}\cdot\left(v_{a_1^*(k)}-s_{a_2^*(k)}\right)^2\right)^{\frac{1}{2}}\end{aligned}\tag{1}$$

where $\hat{d}$ represents the Dynamic Time Warping (DTW) [8], a^* denotes the optimal alignment of the two segments v and s. k is the index variable, and p denotes the total number of components. (1) can be intuitively interpreted as projecting the weights onto the positions aligned by DTW.

Since Shapelets may exhibit different feature representations at different time periods, weights across time segments are introduced to quantify these variations. The global factor u captures the cross-segment influence and is added to the model as an adjustment parameter, and the distance between Shapelets v and time series T can be revised as follows:

$$\hat{D}(x,T|w,u)=\min_{1\leqslant k\leqslant m} u_k\cdot\hat{d}(v,s_k|w)\tag{2}$$

where T is divided into m equal-length segments, *i.e.*, $T=\{s_1,...,s_m\}$. (2) represents the time-aware perceived distance between specific Shapelets and time series segments.

The local and global factors of each Shapelet can be learned under appropriate criteria. By combining (1) and (2), (3) is derived as:

$$\hat{\mathcal{L}}=-g(S_{_{pos}}(v,T),S_{_{neg}}(v,T))+\lambda\|w\|+\epsilon\|u\|\tag{3}$$

where $\hat{\mathcal{L}}$ denotes the difference between positive and negative samples and the specified Shapelets v, $S_*(v,T)$ represents the set of distances between v and T, and $g(\cdot,\cdot)$ calculates the scalar distance between the two distance sets. Additionally, λ and ϵ are penalty hyperparameters in the learning process. This work employs the proposed time-aware Shapelets extraction algorithm to identify the most representative time-aware Shapelets from the candidate pool, which serves as the foundation for constructing the evolution graph. Specifically, for each candidate Shapelet in the pool, its local factor w_i and global factor u_i are initialized. Then, the Adam optimizer is used along with the loss function $\mathcal{L}_i$ in (3) to determine the optimal values of w_i and u_i. Finally, the top K Shapelets with the lowest loss values are selected as the final output.

D. Time-aware Shapelets evolution graph

After obtaining the time-aware Shapelets, STEG employs an evolution graph to capture and display their co-occurrence and sequential relationships. The definition of the Shapelets evolution graph is shown in (4).

$$\mathcal{G}=(\mathcal{V},\mathcal{H},\mathcal{E}\mid\Theta)\tag{4}$$

The Shapelets graph is a directed, unweighted graph with parameter set Θ, where $\mathcal{V}$ consists of K nodes, each representing a temporal Shapelet. $H=h_1,\ldots,h_{|\mathcal{V}|}\in\mathbb{R}^{|F|}$ represents the nodes v_i in F-dimensional space. The edges of the graph are denoted by $e_{ij}\in E$, which represent the transition relations between nodes v_i and v_j, *i.e.*, the temporal relationship between two Shapelets. The weight of the edge is computed by $f(i,j|\mathcal{H},\mathcal{E},\Theta)$, where $f(\cdot)$ refers to the attention mechanism used to model pairwise dependencies.

The first step in constructing the Shapelets evolution graph is to initialize the parameters. First, the edge weights for each time series sample are computed. Next, all possible transitions between time-aware Shapelets are calculated. The intrinsic information of the original time series is embedded into the evolution graph to initialize the node features. Therefore, the distance feature of Shapelets v on time series $T=\{s_1,...,s_m\}$ is defined as in (5).

$$h_i=\mathrm{O}(d(v_i,s_j),1\leqslant j\leqslant m)\tag{5}$$

where O represents concatenation, indicating that multiple values are joined together to form a single vector. The second step involves modeling the transition relationships between time-aware Shapelets using a graph attention network. This transformation converts the time series classification task into a graph classification task, enabling the model to learn transition relationships and weights between pairs of time-aware Shapelets. Given a Shapelets evolution graph $\mathcal{G}(\mathcal{V},\mathcal{H},\mathcal{E}\mid\Theta)$, the attention score between nodes v_i and nodes v_j can be defined as in (6) and (7).

$$e_{ij}=\mathrm{LeakyReLU}\left(\alpha^T\left[Wh_j\|Wh_i\right]\right)\tag{6}$$

$$\alpha_{ij}=\mathrm{Softmax}\left(e_{ij}\right)=\frac{\exp\left(e_{ij}\right)}{\sum_{k\in N_i}\exp\left(e_{ik}\right)}\tag{7}$$

where $\mathrm{LeakyReLU}$ and $\mathrm{Softmax}$ denote the activation functions. h_i and h_j represent the updated and original node features, respectively.

In the graph attention network, $\Theta=\{W,\alpha\}$ denotes the parameters of the self-attention mechanism, implemented via a single-layer feedforward neural network. e_{ij} measures the

importance of node v_i to node v_j. After normalizing e_{ij}, the attention coefficients α_{ij} are obtained. These attention parameters are learned through a graph classification task. Multihead attention with n heads captures diverse relationships between nodes, and node-level hidden features are represented by (8). Finally, (9) illustrates that the transition graph feature extracted from the given time series is obtained by averaging all node hidden features, effectively capturing the overall evolutionary trends of the temporal patterns.

$$\hat{h}_i = \Big\|_{k=1}^{n} \sigma\Big(\sum_{j\in N_i} \alpha_{ij}^k W^k h_j\Big) \tag{8}$$

$$\hat{\mathcal{H}} = \sum_{i=1}^{K} \frac{1}{K} h_i = \sum_{i=1}^{K} \frac{1}{K} \Big\|_{k=1}^{n} \sigma\Big(\sum_{j\in N_i} \alpha_{ij}^k W^k h_j\Big) \tag{9}$$

To train STEG, it processes the graph features using Softmax and MLP to predict the labels, with cross-entropy as the loss function. It is defined as:

$$\mathcal{L} = \text{CrossEntropy}\left(\text{Softmax}\left(\sigma\left(MLP\left(\mathcal{H}\right)\right)\right), y\right) \tag{10}$$

where σ represents the activation function, and y denotes the anomaly labels in the water quality time series. This processing yields the Shapelets state transition graph derived from the original water quality time series, enabling feature extraction and modeling, while providing deeper insights into the patterns of data variations.

E. Representation Learning and Anomaly Classification

After processing the water quality index monitoring time series, the time-aware Shapelets evolution graph is constructed. The extracted features can then be used for downstream tasks. In this work, DeepWalk [9] algorithm is used to generate node embeddings, denoted as $\mu \in \mathbb{R}^B$, where B is the embedding dimension. The paths in the evolution graph represent possible Shapelets transition patterns.

Given the assignment probability set $p_1, ..., p_m$, the vector representation $r(v_{i,j})$ of each Shapelet $v_{i,j}$ is weighted by its assignment probability $p_{i,j}$. Summing over all time segments yields the embedded features for each segment. If a time segment lacks a corresponding Shapelet, its embedding is set to null. Finally, these short embedding vectors are concatenated to form the overall time series representation Φ_t, as shown in (11). The time series with extracted features can then be used for downstream anomaly detection tasks.

$$\Phi_t = \Big(\sum_j p_{i,j} \cdot r(v_{i,j})\Big), 1 \leqslant i \leqslant m \tag{11}$$

IV. Experimental Results and Discussion

A. Dataset and Data Processing

1) Dataset: Publicly available data from national automatic surface water quality monitoring stations in the Beijing-Tianjin-Hebei (BTH) region of China are used in this work. The stations include Wucun and Beijing. The dissolved oxygen (DO) index from the Beijing station, covering April 2, 2014, to September 17, 2018, with 9,778 observations, is analyzed for anomaly detection and time series patterns. Similarly, the total nitrogen (TN) index from the Wucun station, spanning August 31, 2018, to December 12, 2021, with 6,510 observations, is used for analysis. The dataset is split into training and test sets at an 8:2 ratio for model training and evaluation.

2) Data Processing: The raw data from water quality monitoring stations contains missing values due to unpredictable weather, unexpected events, or equipment failures. Linear interpolation is applied to estimate missing values using a linear relationship between known data points. Since the missing values are minimal and sparsely distributed, the simplicity and efficiency of linear interpolation suffice for data imputation. The completed water quality data of the DO indicator from the Wucun Station in the Haihe River Basin are presented in Fig. 2, where abnormal measurements are highlighted by red dots. The data from the Beijing Station and other indicators follow a similar format.

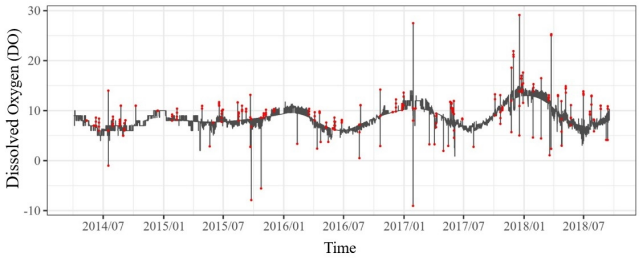

Fig. 2. DO index after data completion treatment

B. Results and Evaluation

Accuracy and F1-Score are employed as evaluation metrics to quantify the discrepancy between anomaly detection results and actual anomalies. Table I presents the performance evaluation of various prediction models for detecting DO and TN content changes at two monitoring stations. The results indicate that STEG excels in both Accuracy and F1-Score across the two datasets. In the DO dataset, both metrics surpass all other models, with significant improvements: Accuracy exceeds the baseline average by 59.1%, and F1-Score by 56.7%. In the TN dataset, Accuracy surpasses all other models by a substantial margin, whereas F1-Score is slightly lower than that of the best-performing AE. Accuracy exceeds the baseline average by 54.1%, while F1-Score improves by 29%. Specifically, compared to Transformer, STEG demonstrates a significantly better ability to model temporal dependencies, which is crucial for anomaly detection in water quality data. Additionally, compared to traditional models, including K-Means, LOF, and RF, STEG exhibits stronger generalization capabilities when handling high-dimensional features, leading to more accurate distinction between normal and abnormal water quality variations. Analysis of Table I indicates that STEG outperforms benchmark models in capturing both normal and abnormal water quality patterns.

C. Model Interpretability Analysis

STEG's key advantage over other models is its ability to explain reasoning process and results using historical

TABLE I
COMPARISON OF MODEL PERFORMANCE ERRORS IN TWO DATASETS

Model	DO Dataset		TN Dataset	
	Accuracy	F1-Score	Accuracy	F1-Score
MGD	0.669	0.604	0.707	0.713
LOF	0.504	0.414	0.714	0.649
K-Means	0.503	0.502	0.436	0.370
KNN	0.670	0.624	0.647	0.615
RF	0.669	0.667	0.583	0.511
LSTM	0.523	0.522	0.631	0.488
AE	0.731	0.732	0.786	**0.737**
VAE	0.522	0.521	0.631	0.488
Transformer	0.523	0.525	0.632	0.494
STEG	**0.985**	**0.780**	**0.988**	**0.726**

data, which is crucial in anomaly detection. This improves model transparency, traceability, reliability, and early warning effectiveness, ultimately enhancing decision-making support. The core of this model is the time-aware Shapelets evolution graph, whose interpretability is analyzed below. Fig. 3 shows the evolution graph of the top 50 representative time-aware Shapelets from the DO monitoring dataset. This directed, weighted graph combines bidirectional edges into a single unweighted edge for readability.

Each node represents a time-aware Shapelet, and each edge denotes a transition between patterns. The out-degrees of a node sum to one, representing the probability of transitions from that Shapelet to others. The size of each node reflects the total degree, which is the sum of its in-degree and out-degree, and also indicates the frequency of the corresponding temporal pattern. A color gradient is used to show the connection strength, with blue-violet for stronger connections and red-orange for weaker ones. In Fig. 3, nodes x2, x3, x28, and x29 have much higher in-degree and out-degree sums compared to other nodes. As shown in Fig. 4, extracting their shapes for analysis reveals stable variations, consistent with the original time series characteristics, where water quality indicators remain mostly stable.

Edge thickness and color intensity represent the probability of pattern transitions in historical data. Thicker, darker edges indicate higher transition probabilities, while thinner, lighter edges represent lower probabilities. Analyzing edge thickness helps capture the frequency of specific transitions, reflecting short-term dynamic dependencies in the time series.

As shown in Fig. 5, the transition sequence x3→x28→x14 occurs more frequently than x3→x28→x44 in Fig. 6, making the probability of pattern evolution a key criterion for identifying anomalous time segments. A detailed analysis is then performed on the time-aware behavior of a specific Shapelet. Taking x29 as an example, Fig. 7 presents its global temporal sensitivity. The heatmap reflects the similarity between the Shapelet and the water quality pattern. Darker colors and values closer to one represent higher similarity. Shapelet x29 is more sensitive from April to September, indicating more frequent occurrence in warmer months. Its sensitivity decreases from October to March, during colder periods. Fig. 2 shows that DO levels are generally lower in summer, which

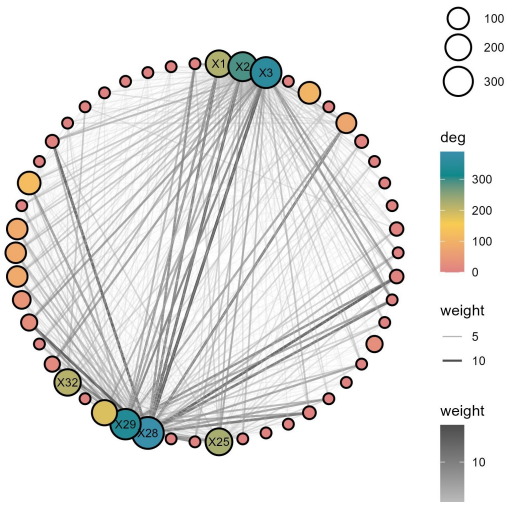

Fig. 3. Time-aware Shapelets evolution graph with 50 nodes

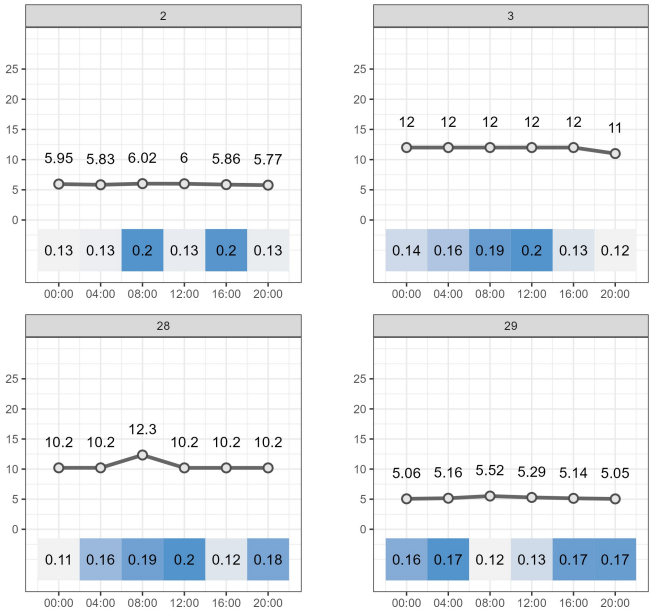

Fig. 4. Time-aware Shapelets at x2, x3, x28, x29

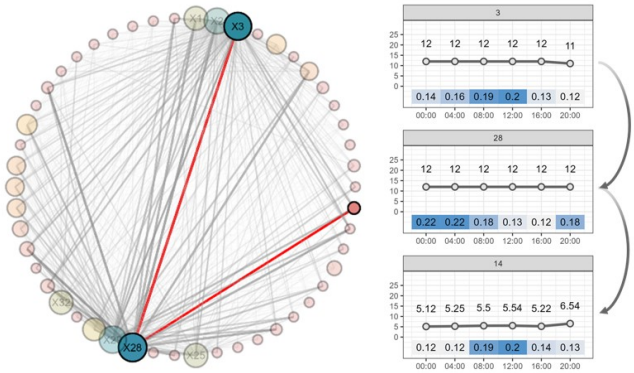

Fig. 5. Transition path of nodes x3→x28→x14

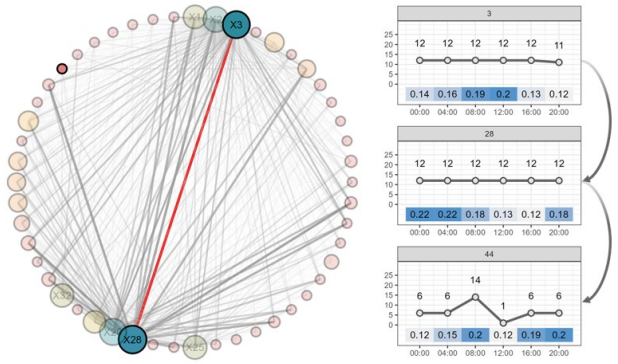

Fig. 6. Transition path of nodes x3→x28→x44

aligns with x29's primary association with low DO values. In contrast, Fig. 8 shows that Shapelet x40 is more active in colder months, corresponding to higher DO levels in winter. These results show that time-aware Shapelets can capture seasonal sensitivity without explicitly modeling periodicity, offering additional insights into water quality dynamics.

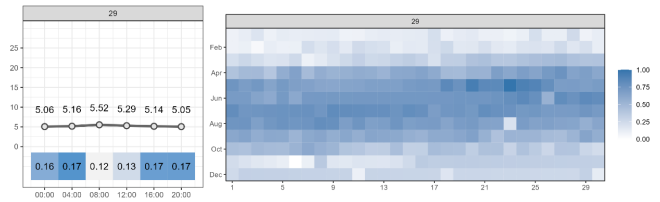

Fig. 7. Time sensitivity of Shapelet x29 throughout the year

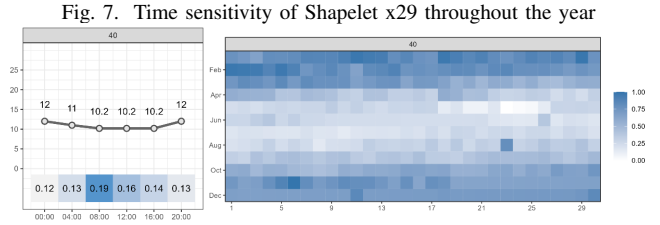

Fig. 8. Time sensitivity of Shapelet x40 throughout the year

V. Conclusion

The growing volume of sensing data and the rising demand for intelligent, transparent water environment management [10] present critical challenges to achieving accurate and interpretable anomaly detection in early warning systems. To address this challenge, this work introduces a water quality anomaly detection model, the Shapelet Temporal Evolution Graph network (STEG), which integrates time-aware Shapelets and graph attention networks. The proposed model retains the interpretability advantages of Shapelet-based methods, while improving dynamic modeling capabilities for water quality time series by incorporating time-awareness into Shapelets and analyzing their evolutionary relationships. This approach enhances information representation, improves detection accuracy, and effectively captures the dynamic characteristics of time series. Experimental results indicate that STEG outperforms both deep learning and traditional machine learning methods while providing strong interpretability that supports understanding and ensures transparency.

In future work, an intelligent optimization algorithm [11]–[13] will be employed to automatically determine the number of representative Shapelets. Preprocessing methods based on decomposition and entropy [14] will also be considered to enhance time series representation. In addition, spatiotemporal modeling [15] will be incorporated by integrating spatial dependencies between water quality monitoring stations.

References

[1] J. Bi, M. Yuan, H. Yuan, Z. Wang and J. Qiao, "Water Quality Anomaly Detection with Dual Sliding Windows and Convolutional LSTM," *2024 IEEE International Conference on Systems, Man, and Cybernetics (SMC)*, Kuching, Malaysia, 2024, pp. 3559–3564.

[2] F. Wu, R. Jing, X. -P. Zhang, F. Wang and Y. Bao, "A Combined Method of Improved Grey BP Neural Network and MEEMD-ARIMA for Day-Ahead Wave Energy Forecast," *IEEE Transactions on Sustainable Energy*, vol. 12, no. 4, pp. 2404–2412, Oct. 2021.

[3] W. Wu, Y. Xia and W. Jin, "Predicting Bus Passenger Flow and Prioritizing Influential Factors Using Multi-Source Data: Scaled Stacking Gradient Boosting Decision Trees," *IEEE Transactions on Intelligent Transportation Systems*, vol. 22, no. 4, pp. 2510–2523, Apr. 2021.

[4] Z. Zhang and X. Huang, "ShapeEvoNet: A shapelet-based Time Series Classification Method," *2023 IEEE 35th International Conference on Tools with Artificial Intelligence (ICTAI)*, Atlanta, GA, USA, 2023, pp. 669–674.

[5] J. Duan, B. Xiao, S. Wang, H. Zhou and X. Liu, "ARISE: Graph Anomaly Detection on Attributed Networks via Substructure Awareness," *IEEE Transactions on Neural Networks and Learning Systems*, vol. 35, no. 12, pp. 18172–18185, Dec. 2024.

[6] Z. Yuan, M. Shao and Q. Yan, "Motif-Level Anomaly Detection in Dynamic Graphs," *IEEE Transactions on Information Forensics and Security*, vol. 18, pp. 2870–2882, May. 2023.

[7] G. Li, B. Choi, J. Xu, S. S. Bhowmick, K. -P. Chun and G. L. -H. Wong, "Efficient Shapelet Discovery for Time Series Classification," *IEEE Transactions on Knowledge and Data Engineering*, vol. 34, no. 3, pp. 1149–1163, Mar. 2022.

[8] R. Sun, Q. Cheng, F. Xie, W. Zhang, T. Lin and W. Y. Ochieng, "Combining Machine Learning and Dynamic Time Wrapping for Vehicle Driving Event Detection Using Smartphones," *IEEE Transactions on Intelligent Transportation Systems*, vol. 22, no. 1, pp. 194–207, Jan. 2021.

[9] H. Yu, R. Ma, J. Chao and F. Zhang, "An Overlapping Community Detection Approach Based on Deepwalk and Improved Label Propagation," *IEEE Transactions on Computational Social Systems*, vol. 10, no. 1, pp. 311–321, Feb. 2023.

[10] J. Bi, Z. Wang, H. Yuan, X. Wu, R. Wu, J. Zhang and M. Zhou, "Long-Term Water Quality Prediction With Transformer-Based Spatial-Temporal Graph Fusion," *IEEE Transactions on Automation Science and Engineering*, vol. 22, pp. 11392–11404, Jan. 2025.

[11] J. Bi, Z. Wang, H. Yuan, J. Zhang, and M. Zhou, "Cost-Minimized Computation Offloading and User Association in Hybrid Cloud and Edge Computing," *IEEE Internet of Things Journal*, vol. 11, no. 9, pp. 16672–16683, May 2024.

[12] H. Zhao, Z. Wang, G. Cheng, W. Qian, P. Chen, J. Yin, S. Dustdar, and S. Deng, "Online Workload Scheduling for Social Welfare Maximization in the Computing Continuum," *IEEE Transactions on Services Computing,* doi: 10.1109/TSC.2025.3570845.

[13] H. Yuan, J. Bi, Z. Wang, J. Yang, and Jia Zhang, "Partial and Cost-minimized Computation Offloading in Hybrid Edge and Cloud Systems," *Expert Systems with Applications*, vol. 250, no. 15, pp. 1–13, Sept. 2024.

[14] H. Yuan, Q. Hu, M. Wang, S. Wang, J. Bi, *et al.*, "Data-Filtered Prediction With Decomposition and Amplitude-Aware Permutation Entropy for Workload and Resource Utilization in Cloud Data Centers," *IEEE Internet of Things Journal*, vol. 12, no. 12, pp. 19189–19201, Jun. 2025.

[15] J. Bi, X. Wu, H. Yuan, Z. Wang, D. Wei, R. Wu, J. Zhang, J. Qiao and R. Buyya, "STMF: A Spatio-Temporal Multimodal Fusion Model for Long-term Water Quality Forecasting," *IEEE Internet of Things Journal*, doi: 10.1109/JIOT.2025.3581282.